

# Study of the Surface Adhesion of Pressure-Sensitive Adhesives by Atomic Force Microscopy and Spherical Indenter Tests

Adriana Paiva, Nina Sheller, and Mark D. Foster\*

*Maurice Morton Institute of Polymer Science, The University of Akron, Akron, Ohio 44325-3909*

Alfred J. Crosby and Kenneth R. Shull

*Department of Materials Science and Engineering, Northwestern University, Evanston, Illinois 60208*

*Received May 17, 1999; Revised Manuscript Received December 8, 1999*

**ABSTRACT:** Atomic force microscopy allows observation of the adhesive surface and characterization of the adhesive behavior on a nanoscale level, providing new and important information about the behavior of pressure-sensitive adhesives (PSAs). In this research PSAs consisting of poly(ethylene propylene) and the *n*-butyl ester of abietic acid are studied. Results of nanoindentation measurements indicate two different types of behavior: a viscoelastic behavior in the tackifier-rich domains and a more highly dissipative response in the matrix with a gradual transition behavior in areas close to the interfaces between the domains and the matrix. The adhesive energy appears to be dictated predominantly by the tackifier-rich domains.

## Introduction

Pressure-sensitive adhesives (PSAs) have been defined as materials that will wet a surface quickly when a light pressure has been applied and will resist detachment with clean removal. These special properties are obtained by mixing high molecular weight elastomers with small bulky molecules called tackifiers.<sup>1–5</sup> A fundamental understanding of the mechanisms by which these tackifiers modify the properties of elastomeric-based adhesives is still lacking. Bulk properties of PSAs have been studied over the past four decades in an attempt to explain the performance of these systems. Several researchers<sup>1–5</sup> have proposed mechanisms of tackification, but none of them can be used to universally explain tack. More recent measurements have sought to elucidate connections between overall adhesive performance and properties on a more local scale near the surface. These efforts have focused on measuring tackifier composition profiles near surfaces<sup>6</sup> and probing the full adhesive response of the surface over areas of a few mm<sup>2</sup> using devices akin to that used in Johnson–Kendall–Roberts experiments with elastic materials.<sup>7–10</sup> These techniques are powerful tools to understand the tackification mechanism because they allow one to focus on effects important right at the surface as distinct from bulk viscoelastic effects.

This paper extends the concept of probing local adhesive behavior to a still smaller scale (contact areas of ca.  $\mu\text{m}^2$ ) by using the tip of an atomic force microscope (AFM) as the probe. This allows one to measure differences in behavior among the regions of a two-phase adhesive. Vanlandingham<sup>11</sup> and Toikka<sup>12</sup> have looked at homogeneous systems with related techniques. The spherical indenter and AFM approach share several similarities but differ in the magnitudes of contact area, force, and penetration depth characteristic of these two experiments. The forces probed with AFM are on the order of nanonewtons, while those probed with the spherical indenter are on the order of millinewtons. Penetration depths are only several nanometers for

AFM but several microns for the spherical indenter. A very brief comparison of the results from these two different types of measurements provides a preliminary suggestion as to which phase (if either) dominates the surface adhesion in a two-phase system.

## Experimental Section

**Sample Materials and Preparation.** Poly(ethylene propylene) (PEP) with a weight-average molecular weight of 244 000 and a polydispersity index of 1.7 was used as the rubber component. It was obtained by the diimide hydrogenation of the polyisoprene. The *n*-butyl ester of abietic acid (n-BEAA) was chosen as a model tackifier because its chemical structure is well-known,<sup>4</sup> it could be readily synthesized,<sup>6,13</sup> and it belongs to the family of wood rosin derivatives widely used in commercial tackifiers. Surface adhesion measurements were performed on blends of PEP/n-BEAA over the whole range of composition: 10–80 wt %. This adhesive shows a two-phase morphology at room temperature as observed by optical microscopy.<sup>13</sup> These samples were prepared by solution casting on microscope slides using an Accu Gate fluid spreader. Film thickness ranged between 2 and 3 mil (50–75  $\mu\text{m}$ ).

**AFM Measurements.** Atomic force microscopy measurements were performed using the Autoprobe M5 (Park Scientific Instruments). AFM experiments allowed the determination of the film's adhesive properties as well as the study of the topography of the samples. Topographic and friction images of the samples' surfaces were obtained under ambient conditions in contact mode according to established procedures.<sup>14–16</sup> Lateral force microscopy (LFM) measures the lateral deflections or twisting of the cantilever. These deflections usually come from two sources: changes in surface friction and changes in slope. In the first case, the tip may experience greater friction when it passes through some areas in the sample, causing the cantilever to twist more strongly. In the second case, the cantilever twists when it passes over a steep slope. To separate one effect from the other, LFM and AFM images should be collected simultaneously. Also, LFM scans should be acquired in two directions (left to right and right to left). When there are variations in surface friction, the image in one direction is inverted from that in the other direction, while when there are variations only in slope the same image is obtained in both directions.

Local adhesive and viscoelastic properties were measured by indenting the surface with the tip at different points along

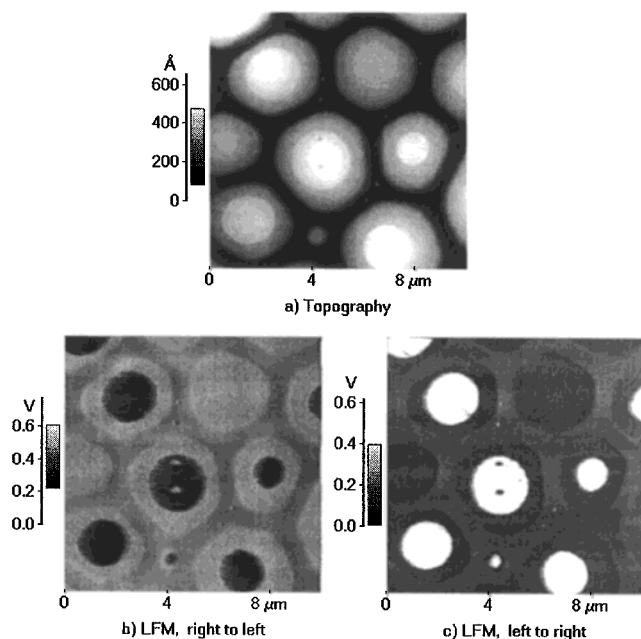


**Figure 1.** Example of images acquired in contact mode for PEP/80 wt % n-BEAA. Samples were 7 months old. (a) Topographic image: bright areas represent high topographic features. (b) LFM image, right to left: dark areas represent high surface friction regions in the sample. (c) LFM image, left to right: bright areas represent high surface friction regions.

a line and recording cantilever deflection as a function of tip to sample distance (force–distance measurements).<sup>14–16</sup> Each line was chosen to begin inside a tackifier-enriched domain and cross over into the matrix as illustrated in the inset of Figure 3. Measurements were performed at a displacement rate of 2.5  $\mu\text{m/s}$ . Silicon probes (Ultralever, Park Scientific Instruments) with V-shaped cantilevers and conical tips with typical radius of curvature  $\sim 10$  nm were used for all measurements. For a quantitative study of the adhesion forces, precise values of both the cantilever deflection and spring constant were indispensable.<sup>17–19</sup> The spring constant of the cantilevers was experimentally determined to be  $0.41 \pm 0.03$  N/m following the procedure described by Tortonese et al.<sup>19</sup>

**Adhesive Measurements with a Spherical Indenter.** Spherical indenter experiments were performed as described

recently.<sup>10</sup> The adhesives were pressed against a glass hemisphere with a radius of 3 mm at a displacement rate of 2.5  $\mu\text{m/s}$ . When the maximum load was reached (25 mN), the sample was held in contact with the hemisphere for one second, after which unloading started at the same rate of displacement.

## Results and Discussion

**Topography and Surface Friction.** An example of a topographic image in contact mode of the blend of PEP/80 wt % n-BEAA is shown in Figure 1a. At the moment this image was taken, the sample had been cast for 7 months. It can be observed that the domains appear to extend above the matrix, reflecting the fact that the matrix deforms more readily than do the domains. The domains' heights may be accentuated due to two effects: differences in the moduli of the domains and the matrix and differences in solvent evaporation rate between the two phases. This last effect has been reported by others<sup>20</sup> for polymer/polymer blends. Differences in friction between the domains and matrix can be clearly observed in the LFM images (Figure 1b,c). In the image acquired scanning from left to right, the dark areas represent regions of low friction while the bright ones represent regions of high friction. On the other hand, the opposite is true for the image acquired from right to left. From these images it may be inferred that the domains are tackifier-enriched (having the higher friction) while the matrix is polymer-enriched. A preferential dissolution of the tackifier-enriched phase was performed using acetone and confirmed that the domains were tackifier-enriched.

Preliminary results of topographic measurements of blends at other compositions show differences in the structure with composition and time. Figure 2 shows topographic images of PEP/n-BEAA blends at several compositions when the samples were 7 months old. All the blends but PEP/60 wt % n-BEAA showed lateral surface segregation. It is important to mention that optical microscopy observations<sup>13</sup> showed a two-phase morphology for the blends at compositions above 15 wt % n-BEAA, including PEP/60 wt % n-BEAA as well. Thus, the homogeneous surface observed for PEP/60 wt % tackifier reflected the presence of a *surface layer*. On

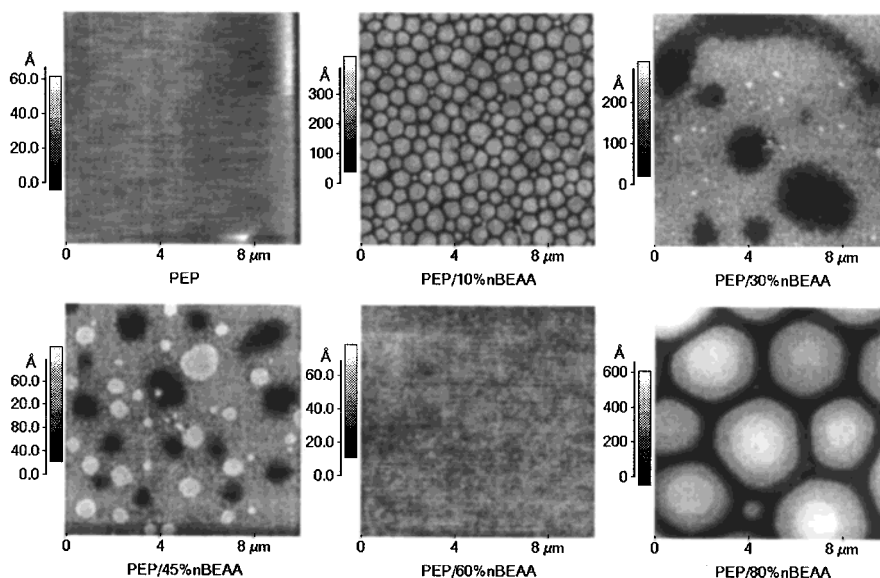


**Figure 2.** Example of topographic images acquired in contact mode for PEP/n-BEAA at several tackifier compositions. Samples were 7 months old.

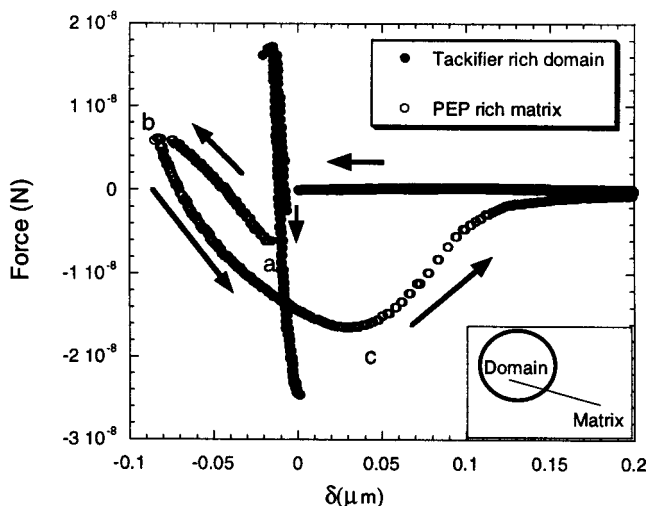


**Figure 3.** Force–displacement curves of PEP/80 wt % n-BEAA obtained from AFM measurements at  $2.5 \mu\text{m/s}$ . Curves have been corrected to show actual separation between the tip and the sample. Two behaviors are observed: a viscoelastic response in the domains and a viscous behavior in the matrix. The inset shows schematically the line along which the measurements were taken.

the other hand, the sample of PEP/10 wt % n-BEAA showed a homogeneous structure by optical microscopy. This is due to the fact that the very small domains of this formulation, which are  $0.5 \mu\text{m}$  in diameter, cannot be resolved by optical microscopy. An aging of the structure over months was observed for the surface structure of these blends, except for PEP/60 wt % n-BEAA, which remained unchanged. Other experiments and the analysis of the  $F$ – $\delta$  curves at several aging times are being undertaken to characterize this time and composition dependence.

**Force–Distance Curves.** Three force–distance curves obtained by indenting the PEP/80 wt % n-BEAA blend with an AFM tip are shown in Figure 3. The primary features of these curves can be highlighted using the curve of the PEP-enriched matrix (open circles) as an example. The cantilever starts above the surface. There is no deflection of the cantilever, and zero force is recorded. As the tip is brought closer to the surface, it jumps into contact at point “a” (snap-in force). Once in contact with the sample, the cantilever’s deflection will increase as sample and cantilever are closer to each other. If the cantilever is sufficiently stiff, the probe tip may indent the surface. In this case the slope of that part of the curve corresponding to contact can provide information about the stiffness of the sample. After loading the cantilever to a desired force (point “b”) the process is reversed, passing through the point of minimal force (point “c”). The difference between this minimal force and the zero force is defined as the snap-out force or adhesive force.

Two types of behavior are observed: a viscoelastic behavior within the domains and a more dissipative response in the matrix, which is rich in polymer. A gradual transition in behavior is observed in areas close to the edges of the domains. While the snap-out in the domains is sudden, this is not the case in the matrix where strong bulk deformation is observed. The shape of the  $F$ – $\delta$  curve for the “interface” varies gradually from that characteristic of the tackifier-enriched domains to that characteristic of the matrix as the point of study moves from the domain to the matrix. The

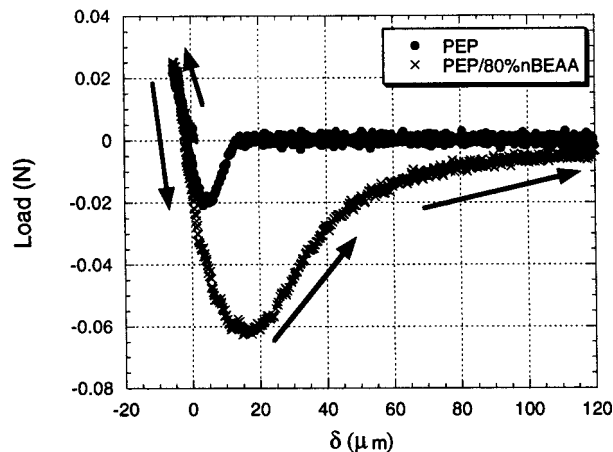


**Figure 4.** Load–displacement curves obtained from spherical indenter tests for PEP and PEP/80 wt % n-BEAA. The slope of the loading curve is related to the stiffness of the material. The area under the curve is proportional to the adhesion energy.

slopes of the loading part of the curves indicate that the tackifier-enriched phase is stiffer than the polymer-enriched matrix at this temperature. The tackifier does not simply act as a plasticizer but has a more complicated effect on the viscoelastic behavior of the adhesive.

The load–displacement curves obtained by measurements with a spherical indenter are presented in Figure 4 for comparison. It is important to mention that all the samples showed a fluidlike behavior. Thus, theories developed for elastic materials cannot be applied. Nevertheless, qualitative information about the stiffness of the sample can be obtained from the slope of the loading portion of the curve. This system shows a slight increase of the laterally averaged stiffness with overall tackifier composition. For both techniques, the area enclosed by the curves is dictated by the amount of energy required to break the adhesive bond. Values for the overall work of adhesion are obtained by dividing this energy by the maximum contact area established during the loading portion of the test. In the spherical indenter test the contact area is monitored constantly and videotaped during the experiment. The contact area for this case is well-defined and measurable. The value of the energy per unit area for the pure polymer, as measured by the spherical indenter, is  $1.1 \pm 0.3 \text{ J/m}^2$ . Adding 80 wt % tackifier increases this value to  $28.2 \pm 3.6 \text{ J/m}^2$ . This value is typical of what it is generally observed with PSAs.<sup>21</sup>

For AFM experiments the maximum contact can only be estimated, and a detailed analysis of the results is not possible. The important issue with respect to this paper is that the volume probed by the AFM experiments is much smaller than the volume probed by the spherical indenter. An estimate of the relevant length scale for AFM experiments can be obtained by assuming that the dissipated energy per unit area for the pure PEP is the same for both experiments. The total dissipated energy measured by AFM for the PEP sample is  $1.3 \times 10^{-15} \text{ J}$ . If we assume that the dissipated energy per unit area is the same as that obtained by the spherical indenter, we can obtain an effective radius of contact,  $a_{\text{max}}$ , for the AFM data. By equating  $1.1 \text{ J/m}^2$  with  $1.3 \times 10^{-15} \text{ J}/\pi a_{\text{max}}^2$ , we obtain  $a_{\text{max}} = 20 \text{ nm}$ .

The value of  $a_{\text{max}}$  that we calculate in this way is consistent with a rough estimate obtained by considering the detailed tip geometry. The shape of the tip as



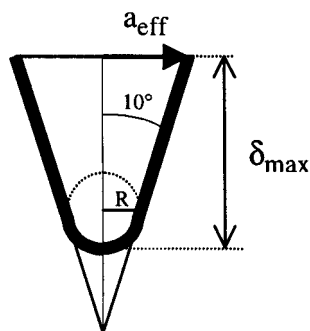


**Figure 5.** Shape of the tip and geometrical considerations in the estimation of the effective contact radius,  $a_{\text{eff}}$ .

reported by the manufacturer is a blunt cone with a half opening angle,  $\phi$ , of  $10^\circ$ . As illustrated in Figure 5, the end of the tip has a radius of curvature,  $R$ , of 10 nm. As an approximation for  $a_{\text{max}}$ , we take the radius of the tip cross section at a distance  $\delta_{\text{max}}$  into the sample, where  $\delta_{\text{max}}$  is the maximum penetration depth established during the loading portion of the test. For values of  $\delta_{\text{max}}$  that significantly exceed  $R$ ,  $a_{\text{max}}$  is given approximately by  $\delta_{\text{max}} \tan \phi$ . For the pure PEP sample with  $\delta_{\text{max}} = 88$  nm (which is indeed substantially larger than  $R$ ), we obtain  $a_{\text{max}} = 16$  nm, which is close to the value of 20 nm calculated above. Several issues need to be kept in mind when making the comparison between the AFM and spherical indenter results. First, the value of  $a_{\text{max}}$  calculated from this geometrical argument is only approximate. Use of the more detailed expression for the Hertzian (nonadhesive) contact between a blunt, rigid cone and an elastic half space gives a lower estimated value of  $a_{\text{max}}$ .<sup>22</sup> Adhesive forces will increase  $a_{\text{max}}$  in a manner that is difficult to quantify in the absence of more extensive measurements. It is for this reason that we do not attempt to quantify the overall work of adhesion obtained from the AFM measurements in more detail.

A more significant issue in our analysis concerns our assumption that values of the work of adhesion obtained by the two measurements are similar. The actual value of  $a_{\text{max}}$  obtained from the spherical indenter test exceeds the thickness of the adhesive layer, so the entire thickness of the adhesive is being deformed during the adhesion test. In contrast to this situation, the AFM measurements probe a lateral region that is much smaller than the thickness of the adhesive layer. Thus, the energy dissipated per area will only be equal for the two experiments if this dissipation occurs in a shallow layer near the surface. One expects that the reason the total energy dissipation is smaller for the AFM tests than for the spherical indenter tests is not only a smaller contact area but also a much smaller depth throughout which energy dissipation occurs in the AFM tests. For this reason, a work of adhesion of  $0.9 \text{ J/m}^2$  is an upper bound for the AFM tests, which means that our estimate of  $a_{\text{max}}$  is a lower bound. This is logically consistent with our geometrical argument, since the value of  $a_{\text{max}}$  determined from the projected area of the tip at a depth of  $\delta_{\text{max}}$  is clearly the lowest possible value for  $a_{\text{max}}$ .

## Conclusions

Results obtained from adhesion measurements with an atomic force microscope and with a spherical indenter indicate that the addition of tackifier enhances the adhesive character of pressure-sensitive adhesives,

not only in the bulk but also in the near surface regions as well. The two-phase model PSA measured by AFM was found to show two distinct types of local behavior: a viscoelastic behavior in the tackifier-enriched domains and a viscous response in the matrix. A gradual transition behavior was observed in areas close to the edges of the domains. Adhesion of this tackifier-enriched phase is largely responsible for the overall adhesive performance of this model PSA. This study highlights the capabilities of atomic force microscopy for contributing to adhesion science by providing new and important information on a highly local scale. Future work will include the study of a system that shows good performance as a PSA but differs from the one considered here in that it is miscible over the whole range of composition.

**Acknowledgment.** The authors thank Professor R. P. Quirk, Dr. S. Corona-Galvan, and R. S. Porzio for providing the polyisoprene. The research support from the Army Research Office, Contracts DAAH04-95-1-0562 and DAAG55-97-1-0079 (DURIP), is gratefully acknowledged.

## References and Notes

- (1) Wetzel, F. H. *Rubber Age (N.Y.)* **1957**, *82*, 291.
- (2) Sherriff, M.; Knibbs, R. W.; Langley, P. G. *J. Appl. Polym. Sci.* **1973**, *17*, 3423.
- (3) Class, J. B.; Chu, S. G. *J. Appl. Polym. Sci.* **1985**, *30*, 805.
- (4) Aubrey, D. W. *Rubber Chem. Technol.* **1988**, *61*, 488.
- (5) Hock, C. W.; Abbott, A. N. *Rubber Age (N.Y.)* **1957**, *82*, 471.
- (6) Li, X. Ph.D. Thesis, The University of Akron, 1996.
- (7) Chaudhury, M. K.; Whitesides, G. M. *Langmuir* **1991**, *7*, 1013.
- (8) Creton, C.; Brown, H. R.; Shull, K. R. *Macromolecules* **1994**, *27*, 3174.
- (9) Deruelle, M.; Léger, L.; Tirrell, M. *Macromolecules* **1995**, *28*, 7419.
- (10) Ahn, D.; Shull, K. R. *Macromolecules* **1996**, *29*, 4381.
- (11) Vanlandingham, M. R.; McKnight, S. H.; Palmese, G. R.; Elings, J. R.; Huang, X.; Bogetti, T. A.; Eduljee, R. F.; Gillespie, J. W. *J. Adhes.* **1997**, *64*, 31.
- (12) Toikka, G.; Spinks, G. M.; Brown, H. R. Proceedings of the 22nd Annual Meeting of The Adhesion Society, Feb 21–24, 1999.
- (13) Paiva, A. Master Thesis, The University of Akron, 1997.
- (14) Sarid, D. In *Scanning Force Microscopy: with Applications to Electric, Magnetic and Atomic Forces*, 2nd ed.; Oxford University: New York, 1994.
- (15) Wiesendanger, R. In *Scanning Probe Microscopy and Spectroscopy: Methods and Applications*, 1st ed.; Cambridge University: New York, 1994.
- (16) Magonov, S.; Whangbo, M.-H. In *Surface Analysis with STM and AFM: Experimental and Theoretical Aspects of Image Analysis*, 1st ed.; VCH: New York, 1996.
- (17) Torii, A.; Sasaki, M.; Hane, K.; Okuma, S. *Meas. Sci. Technol.* **1996**, *7*, 179.
- (18) Gibson, C. T.; Watson, G. S.; Myhra, S. *Nanotechnology* **1996**, *7*, 259.
- (19) Tortorese, M.; Kirk, M. *SPIE* **1997**, *3009*, 53.
- (20) Walheim, S.; Böltau, M.; Mlynek, J.; Krausch, G.; Steiner, U. *Macromolecules* **1997**, *30*, 4995.
- (21) Shull, K.; Ahn, D.; Chen, W.-L.; Flanagan, C. M.; Crosby, A. *Macromol. Chem. Phys.* **1998**, *199*, 489.
- (22) Maugis, D.; Barquins, M. *J. Phys. D: Appl. Phys.* **1983**, *16*, 1843.